

See discussions, stats, and author profiles for this publication at: <https://www.researchgate.net/publication/244426066>

Theoretical Prediction on the Synthesis Reaction Pathway of $N_6(C_2H)_6$

ARTICLE in THE JOURNAL OF PHYSICAL CHEMISTRY A · MARCH 2002

Impact Factor: 2.69 · DOI: 10.1021/jp0141833

CITATIONS

22

READS

30

3 AUTHORS:



Jenna L Wang

University of Kansas

43 PUBLICATIONS 513 CITATIONS

SEE PROFILE



Peter L Warburton

Memorial University of Newfoundland

22 PUBLICATIONS 204 CITATIONS

SEE PROFILE



Paul Mezey

Memorial University of Newfoundland

383 PUBLICATIONS 6,034 CITATIONS

SEE PROFILE

Theoretical Prediction on the Synthesis Reaction Pathway of N_6 (C_{2h})

Li Jie Wang, Peter Warburton, and Paul G. Mezey*

Department of Chemistry, University of Saskatchewan, 110 Science Place, Saskatoon, SK, S7N 5C9, Canada

Received: November 14, 2001; In Final Form: January 16, 2002

The relevant part of the potential energy surface (PES) of reaction leading to N_6 (C_{2h}) synthesized from HN_3 and N_3F was investigated. The structures involved on the PES of N_6 were optimized by hybrid density functional theory method. Relative energies were also calculated using coupled cluster single and doubles (CCSD) theory. The barrier height of the synthesis reaction pathway was predicted to be 27.0 kcal/mol at the level of CCSD/6-311++G**//B3LYP/6-311++G**. Because of the sizable barrier and exothermicity, the experimental synthesis of this compound is challenging, but perhaps feasible. The electron densities of these molecules on the PES were calculated, and the results agree with those of natural bond orbital (NBO) analysis. The calculation results provide the theoretical foundation of a suggestion for the experimental synthesis of N_6 as a high energy density material.

Introduction

Polynitrogen molecules are of interest as high energy-density materials (HEDMs), and as such many stable structures of all-nitrogen clusters have been predicted theoretically. Several isomers of N_6 (with symmetry D_2 , C_{2v} , D_{3h} and two types C_{2h}) have been studied theoretically^{1–12} but few have been studied experimentally.¹³ The focus of theoretical investigations is the stability of N_6 isomers, where the predictions strongly depend on the choice of theoretical method and basis set. Five structures were studied by ab initio Hartree–Fock (HF) and second-order Møller–Plesset (MP2) methods of theory by Engelke.¹ Structures with C_{2v} and D_{3h} symmetry both are minimum points, whereas the structure with C_{2h} symmetry is a transition state at the MP2 level of theory. The hexaazabenzene molecule with D_{6h} symmetry was predicted to be at a minimum point using the restricted Hartree–Fock (RHF) method, but to be a higher-index saddle point on the potential energy surface (PES) of MP2.¹ Another similar result was obtained by Lauderdale and co-workers.⁴ The D_2 structure is a minimum at MP2 theory, as was reported by Glukhovtev and Schleyer² and by Ha and Nguyen.⁵ Tobita and Bartlett's investigation¹² confirmed the saddle point D_{6h} , and the minimum point D_2 structures.

The open chain structure of diazide has been studied for this elusive molecule with various symmetries. Engelke¹ reported that an isomer of N_6 with C_i symmetry is at a minimum at the HF/4-31G* level and a transition state (TS) at the HF/4-31G and MP2/4-31G* levels. The N_6 structure with C_2 symmetry is a minimum by HF method with 4-31G and 4-31G* basis sets, but is a TS at the MP2/4-31G* level. Ha and Nguyen⁵ predicted that the C_{2h} structure is also a TS. The investigation done by Glukhovtsev et al.² showed that the structure with C_2 is a minimum and C_{2h} is a TS at the MP2 level. Klapotke¹⁰ also calculated an open-chain N_6 diazide molecule by HF, MP2 and coupled cluster double (CCD) methods. At all levels of theory applied, the structure with C_2 symmetry was found to represent a true minimum. Gagliardi et al.⁹ obtained a minimum structure

with C_{2h} symmetry using CASPT2 method. Their result is consistent with that of Tobita and Bartlett¹² utilizing density functional theory (DFT) and coupled cluster single and doubles with a perturbative inclusion of triples (CCSD(T)) methods. In a word, the most stable structure of N_6 is the open-chain diazide with C_{2h} symmetry.

To investigate the stability of the N_6 molecule, the dissociation pathway of N_6 was studied^{9,11} after its stability was determined. Gagliardi et al.⁹ reported the dissociation pathway of N_6 into three N_2 molecules using multiconfigurational second-order perturbation theory (CASSCF/CASPT2). The computed energy barrier is 28.7 kcal/mol (CASPT2). Our previous works¹¹ showed that the dissociation barrier is 14.4 and 15.4 kcal/mol at the B3LYP/6-31G* and B3LYP/6-311+G* levels, respectively. Wright¹⁴ reported that N_6 is slightly stabilized and can be certainly stable at low temperature.

N_6 isomers are of significant interest as HEDM for propulsion and explosive applications. The critical properties for effective HEDM molecules are the lower synthesis barrier and the higher dissociation barrier. Although N is an isoelectronic analogue to CH and many stable complexes of $(CH)_n$, such as benzene (C_6H_6) and polyalkyne, have been known, most corresponding nitrogen clusters (N_6) have not been prepared. Vogel et al.¹³ did some work on the experimental research of N_6 . In the time since Christe et al.¹⁵ synthesized the AsF_6^- salt of N_5^+ by reaction of $N_2F^+AsF_6^-$ with HN_3 in anhydrous hydrogen fluoride at $-78^\circ C$, some potential energy surfaces on nitrogen clusters have been studied in our previous works.^{16–18} Therefore we designed a possible pathway for synthesizing linear N_6 (C_{2h} symmetry) by HN_3 and N_3F as well, that is, $HN_3 + N_3F \rightarrow N_6 + HF$. The early experimental data of the HN_3 molecule can be obtained elsewhere,^{19–21} whereas the theoretical studies on HN_3 are more recent.^{22,23} The very high heat of formation (about 130 kcal/mol) of fluorine azide (NNNF) makes it a candidate as an energetic material. The stability and its decomposition to N_2 have been studied in a number of experimental and theoretical works.^{24–27}

For the reaction $HN_3 + N_3F \rightarrow N_6 + HF$, according to the character of the reactants, the possible mechanism could be as follows:

* To whom correspondence should be addressed. Fax: 1–306-966-4730. Tel: 1–306-966-4661. E-mail: mezey@sask.usask.ca., wljje@rhodent.usask.ca.

First, HN₃ and N₃F form a molecule-molecule complex 1, via the coulomb force, with no activation energy barrier



Then, the H-F bond forms between the H atom of the HN₃ and the F atom of the N₃F (see Figure 1). At the same time, the N-N bond also forms between the N1 and N2 atoms of the two reactants, leading to another molecule-molecule complex 2 via TS



With the full cleavage of the H...N bond in the complex 2, the complex 2 dissociates into two fragments N₆ and HF



These calculations provide a theoretical suggestion for improved design of the corresponding HEDMs.

Computational Method

The geometries of the reactants, products, transition state, and complexes involved have been optimized with ab initio and DFT methods at the levels of HF/6-31G**, B3LYP/6-31G** and B3LYP/6-311++G**, where B3LYP is a DFT method using Becke's three-parameter nonlocal exchange functional²⁸ with the nonlocal correlation of Lee, Yang, and Parr.²⁹ The designation 6-31G** refers to a standard split-valence double- ζ polarization basis set, while the 6-311++G** is a split-valence triple- ζ polarization basis set augmented with diffuse functions.³⁰ The relative energies were also calculated at the CCSD/6-311++G**//B3LYP/6-311++G** levels. The natural bond orbital (NBO) analysis was calculated at the level of B3LYP/6-31G**. To characterize the nature of the stationary points and determine the zero-point vibrational energy (ZPVE) corrections, harmonic vibrational frequencies were also calculated at the levels of the theory mentioned above. Stationary points were identified as either local minima or transition states. All calculations were carried out with the Gaussian 98 program package.³¹ To confirm that a given transition state connects reactants and products, minimum energy path calculations³²⁻³⁶ were performed at the above levels with a coordinate stepsize of 0.1 (amu)^{1/2}bohr.

The electron densities of species involved on the potential energy surface were calculated and analyzed using RHO-CALC2000³⁷ and MOLCAD II module³⁸⁻⁴⁰ of the SYBYL molecular modeling package.⁴¹

Results and Discussion

1. PES of the Synthesis Reaction. The relative energies corrected by ZPVE of the reactants, products, transition state, and complexes (1 and 2) are given in Table 1. In the following discussions, we will mainly use the B3LYP/6-311++G** results unless otherwise indicated.

The starting point in the mechanism is the formation of a molecule-molecule complex 1 (see Figure 1). According to the charge distributions calculated at the levels of HF/6-31G**, B3LYP/6-31G** and B3LYP/6-311++G** theory, the positive charges mostly concentrate on the H atom of HN₃, whereas the negative charges mainly concentrate on F atom of N₃F. When the two molecules collide, the H atom of HN₃ mainly attacks the F atom of N₃F, via long-range coulomb force. Therefore, the complex 1 can be formed with no activation energy barrier. As shown in Figure 1, the complex 1 has C₁ symmetry with a long bond length of H-F (2.296 Å), and its relative energy 1.5

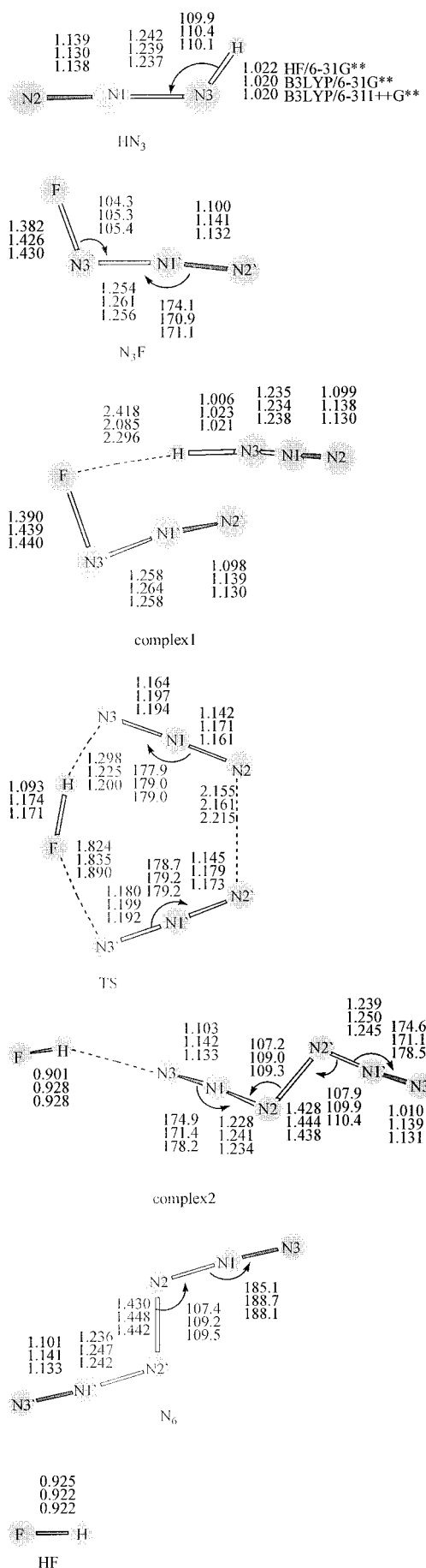


Figure 1. Geometric parameters for various structures involved in the PES.

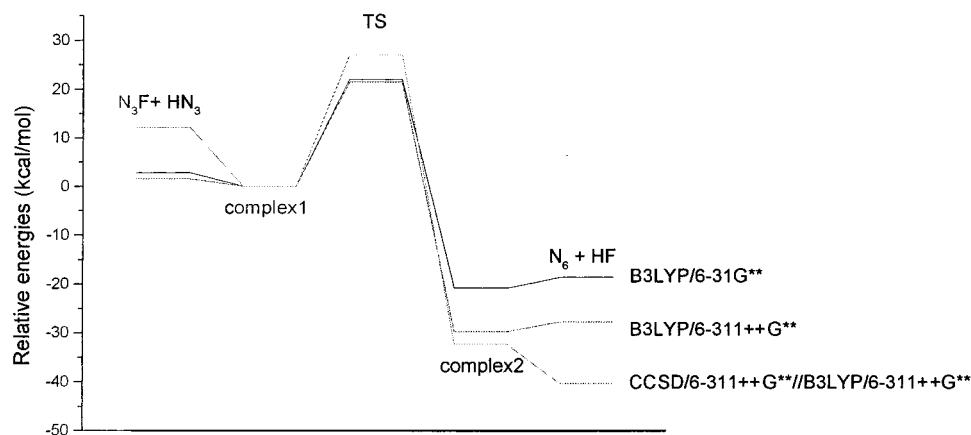


Figure 2. Energy variations along the potential energy surface of the N_6 synthesis reaction at the three levels.

TABLE 1: Relative Energies (kcal/mol, corrected by ZPVE) of Species on the N_6 PES

	HF 6-31G**	B3LY 6-31G**	B3LY 6-311++G**	CCSD ^a
$N_3F + HN_3$	1.7	2.8	1.5	12.1
complex 1	0.0	0.0	0.0	0.0
TS	59.8	22.0	21.4	27.0
complex 2	-25.6	-20.8	-29.7	-32.3
$N_6 + HF$	-24.4	-18.6	-27.7	-40.3

^a Calculated at the CCSD/6-311++G**//B3LY/6-311++G** level.

kcal/mol, approaching that of the reactants ($HN_3 + N_3F$). The complex 1 is a local minimum (Figure 2) on the PES for it has all real harmonic vibrational frequencies at all levels of theory employed.

Following the complex 1, a transition structure (TS, see Figure 1) is found, in which the distance between the H atom and the F atom is reduced to 1.171 Å, and the distance between the N2 atom and the N2' atom is lengthened to 2.215 Å. In the transition structure, the bond distances of N3'–F and N3–H are lengthened, whereas the distance of F–H and N2–N2' become shorter, and then they form an eight-membered ring structure. This transition structure was verified as being a saddle point of index 1 on the PES for it has one imaginary vibrational frequency with a value of $1069i\text{ cm}^{-1}$. On the basis of the energy difference between the complex 1 and the TS (see Figure 2 and Table 1), the potential energy barrier heights of the reaction corrected by ZPVE were predicted to be 59.8, 22.0, 21.4, and 27.0 kcal/mol at the levels of HF/6-31G**, B3LYP/6-31G**, B3LYP/6-311++G**, and CCSD/6-311G**//B3LYP/6-311++G**, respectively. It is obvious that the HF level is not sufficient to describe this reaction properly, and accounting for electron correlation effects is necessary. Therefore, we omitted the results of HF in Figure 2.

Along the PES of N_6 , when the N2–N2' bond fully formed, another molecule–molecule complex 2 was found (see Figure 1), in which the bond distance between the N2 and the N2' atoms was reduced to 1.438 Å, a distance almost the same as it should be in N_6 diazide (as shown in Figure 1). On the other hand, the N3–H and N3'–F bonds are fully broken. The bond distance between the F atom and the H atom in complex 2, is 0.928 Å, the value of which is also very close to the experimental value of H–F, 0.917 Å.⁴²

To verify that the transition state really connects complex 1 and complex 2, a calculation of the intrinsic reaction coordinate (IRC) was also performed starting from each corresponding transition state at the levels HF/6-31G** and B3LYP/6-31G**, respectively. The geometries of the two complexes (1 and 2)

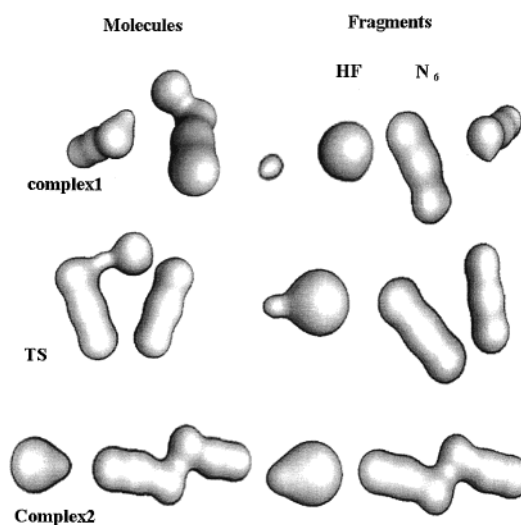


Figure 3. Approximate isodensity surfaces constructed using the RHOCALC2000 program for the value 0.1au of threshold density for the complexes, TS, and their fragments on the PES.

obtained from these IRC calculations are very close to those from the geometry optimization calculations.

The full cleavage of the N3–H bond leads to the formation of the reaction products (N_6 and HF). The optimized geometries of the products are also given in Figure 1. The hexaazadiazide N_6 has C_{2h} symmetry. The relative energy of the product ($HF + N_6$) is -40.3 kcal/mol at the level of CCSD/6-311G**//B3LYP/6-311++G**. Therefore, the synthesis of the N_6 cluster by N_3F and HN_3 is an exothermic reaction. Calculations predict the exothermicity of the whole reaction as being $24\sim 41\text{ kcal/mol}$, so it seems that synthesizing N_6 should be performed at low temperature due to its exothermicity and the low barriers of N_6 dissociating to $3N_2$.^{9,11} Therefore, considering the moderate barrier (27.0 kcal/mol) and exothermicity, the experimental synthesis of this compound is challenging, but perhaps feasible.

2. Analysis of the Electron Density of the Species on the PES. The fragmentary electron densities of HN_3 , N_3F , N_6 , and HF were calculated at the reactant stage, the complex 1 stage, the transition state, the complex 2 stage, and at the products stage of the reaction as given by the PES. Images of the electron densities as 0.1 au isodensity contours are presented in Figures 3 and 4.

As the reaction proceeds along the PES from the complex 1 \rightarrow transition state \rightarrow complex 2, the change in the electron density of the N_3F and HN_3 fragments is visually apparent in the Figures. The electron density between atoms F and N3' in

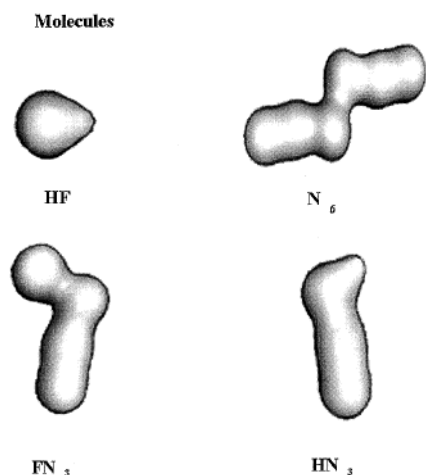


Figure 4. Approximate isodensity surfaces constructed using the RHOCALC2000 program for the value 0.1au of threshold density for reactants and products on the PES.

N_3F has visibly reduced by the time the reactants have reached the transition state, whereas the same can be said for atoms H and N3 in HN_3 . Additionally, electron density has increased between atoms F and H at the transition state. However, on the basis of visual evaluation of the isodensity contour presented at the transition state, it is not possible to comment on whether an increase in electron density has occurred between atoms N2 and N2'.

At the complex 2 stage of the reaction, the HF fragment visually appears indistinguishable from molecular HF, indicating that the N_3-H and $N_3'-F$ bonds have effectively been broken, and the HF bond has formed. The N_6 fragment also appears visually very similar to the calculated molecular counterpart, indicating that the bond formation between N2 and N2' is essentially complete. Further concentrating on the N_6 fragment, it can be seen that the electron density between atoms N2 and N2' is less than that between N2' and N1', which itself is more than that between N1' and N3'. This is a physically sound reflection of the idealized concept of bond order in fragment N_6 : triple, double, and single bonds, respectively. The high electron density can be interpreted as high bond order. This ordering of electron density also implies that if N_6 were to decompose, atoms N1' and N2' would most likely retain their bond to each other, at the expense of the $N_3'-N1'$ bond. By symmetry, the same would be true for atoms N1 and N3. Thus, decomposition could reasonably be expected to result in 3 N_2 molecules. The changes of electron density on fragments show that the bonds form or break during the reaction process.

The results of the visual electron density analysis, which agree with both the IRC study and NBO analysis, offer evidence to show the shape change of fragments during the reaction process. However, visual evaluation of electron density is a subjective process and can be prone error. Therefore, by utilizing the algorithmic Shape Group Method⁴³⁻⁴⁸ shape similarity measure, the confirmation of the visualization process was undertaken. Table 2 shows the shape similarity measures of the various electron density fragments relative to that of the isolated molecules as the fragments occur in each step along the PES.

As the reaction proceeds to the complex 1 stage, notable differences in the shapes of the HN_3 and N_3F molecules occur. The differences are much larger for the N_3F molecule because the electron density of fluorine will tend to dominate that of the molecule. Any change affecting the F atom will be quite notable in the relative shape changes of the molecule as a whole. Thus, at the complex 1 stage, a large electron density change

TABLE 2: Shape Group Similarity Measures for the Electron Density Fragments

	HN_3	N_3F	HF	N_6
starting molecules	1.0000	1.0000		
complex 1	0.7380	0.5886	0.4205	0.6418
transition state	0.6727	0.5065	0.4539	0.7989
complex 2	0.6207	0.4419	0.9248	0.9455
end molecules			1.0000	1.0000

has already occurred due to the Coulombic interaction of atoms F and H. The Coulombic interaction must be the source of the shape changes because very little geometrical change of the nuclear arrangement has occurred in either of the starting molecules. This change is also reflected in the shape change of HN_3 in the complex 1 stage relative to the isolated molecule, but the change is not as large due to the generally lower electron density that was originally present around the H atom. However, at the complex 1 stage, the shape similarity measure of the HF fragment compared to the product molecule is still very low, which means that a formal HF bond has most likely not yet been created.

As the reaction proceeds through the transition state to the complex 2 stage, the electron density of the starting molecules is further changed relative to the original molecules, indicating bond formation and cleavage. The value of 0.7989 indicates that N_6 is becoming a more distinct entity in the transition state, although HF is not, with a value of 0.4539. Because the geometry of the transition state shows that the hydrogen is effectively shared between F and N3, it is expected that the shape of the HF fragment will be quite different than the isolated HF molecule. Such hydrogen sharing, however, does not dominate the shape of the N_6 fragment, and so that fragment should be more similar to isolated N_6 .

By the time the complex 2 stage is achieved, both N_6 and HF are essentially the same as the isolated molecules, indicating that near completion of bond formation and cleavage in the reaction occurs between the transition state and complex 2.

Summary

All of our calculations on the PES related to synthesizing N_6 by HN_3 and N_3F showed that the process is an exothermic reaction. The entire reaction pathway can be outlined as follows: first, N_3F and HN_3 form a molecule-molecule complex, $[N_3F \cdots HN_3]$ (complex 1), via long-range coulomb force, with no activation energy barrier. Then, the distances between the N2 and N2', H and F of the complex 1 were shortened. The full formation of N_2-N_2' and $H-F$ bonds leads to another molecule-molecule complex, $[H-F \cdots N_3-N_3]$ (complex 2). This process involves an eight-membered ring transition structure. With the full cleavage of the $F \cdots N_3'$ and $H \cdots N_3$ bonds, the complex 2 dissociates into two fragments, N_6 and HF. The barrier height of the synthesis reaction pathway was predicted to be 27.0 kcal/mol at the level of CCSD/6-311++G**//B3LYP/6-311++G**. The results of the visual electron density analysis imply the process of species forming on the PES of synthesis pathway of N_6 , confirmed by nonvisual shape group similarity measure analysis. Because of the sizable barrier (27.0 kcal/mol) and exothermicity, the experimental synthesis of this compound is challenging, but perhaps feasible.

It is possible that a condensed phase reaction would eventually be the optional choice. In such a case, the actual charges at various nitrogen atoms in the context of interactions between neighbor molecule will likely become important factors that complicate the problem considerably. In a forthcoming study,

we shall attempt to investigate these effects and do some further investigations of this reaction at other levels of theory.

Supporting Information Available: Table S1 displays the total energies (hartree) and ZPVE (kcal/mol) of species on the N₆ PES. This material is available free of charge via the Internet at <http://pubs.acs.org>.

Acknowledgment. The financial support of the National Sciences and Engineering Research Council (NSERC) Canada, in the form of both operating of strategic research grants to Paul G. Mezey is gratefully acknowledged.

References and Notes

- Engelke, R. *J. Phys. Chem.* **1992**, 96, 10 789.
- Glukhovtsev, M. N.; Schleyer, P. v. R. *Chem. Phys. Lett.* **1992**, 198, 547.
- Engelke, R. *J. Phys. Chem.* **1989**, 93, 5722.
- Lauderdale, W. J.; Stanton, J. F.; Bartlett, R. J. *J. Phys. Chem.* **1992**, 96, 1173.
- Ha, T.-K.; Nguyen, M. T. *Chem. Phys. Lett.* **1992**, 195, 179.
- Harcourt, R. D. *J. Mol. Struct.* **1993**, 300, 245.
- Glukhovtsev, M. N.; Jiao, H.; Schleyer, P. v. R. *Inorg. Chem.* **1996**, 35, 7124.
- Gimarc, B. M.; Zhao, M. *Inorg. Chem.* **1996**, 35, 3289.
- Gagliardi, L.; Evangelisti, S.; Barone, V.; Roos, B. O. *Chem. Phys. Lett.* **2000**, 320, 518.
- Klapotke, T. M. *J. Mol. Struct.* **2000**, 499, 99.
- Li, Q. S.; Wang L. J. *J. Phys. Chem. A*, **2001**, 105, 1203.
- Tobita, M.; Bartlett, R. J. *J. Phys. Chem.* **2001**, 105, 4107.
- Vogel, A.; Wright R. E.; Kenkley, H. *Angew. Chem., Int. Ed. Engl.* **1980**, 19, 717.
- Wright, J. S. *J. Am. Chem. Soc.* **1974**, 96, 4753.
- Christe, K. O.; Wilson, W. W.; Sheehy, J. A.; Boatz, J. A. *Angew. Chem.* **1999**, 38, 2004.
- Xu, W. G.; Li, G. L.; Wang, L. J.; Li, S.; Li, Q. S. *Chem. Phys. Lett.* **1999**, 314, 300.
- Li, Q. S.; Wang, L. J. *J. Phys. Chem. A*, **2001**, 105, 1979.
- Wang, L. J.; Li, S.; Li, Q. S. *Comput. Chem.* **2001**, 22, 1334.
- Eyster, E. H. *J. Chem. Phys.* **1940**, 8, 135.
- Schomaker, V.; Spurr, R. A. *J. Am. Chem. Soc.* **1942**, 64, 1184.
- Amble, E.; Dailey, B. P. *J. Chem. Phys.* **1950**, 18, 1422.
- Zhang, J.; Xu, K.; Amaral, G. *Chem. Phys. Lett.* **1999**, 299, 285.
- Henon, E.; Bohr, F. *Theochem.* **2001**, 531, 283.
- Peters, N. J. S.; Allen, L. C.; Firestone, R. A. *Inorg. Chem.* **1988**, 27, 755.
- Christen, D.; Mack, H. G.; Schatte, G.; Willner, H. *J. Am. Chem. Soc.* **1988**, 110, 707.
- Otto, M.; Lotz, S. D.; Frenking, G. *Inorg. Chem.* **1992**, 31, 3647.
- Chaban, G.; Yarkoy, D. Y.; Gordon, M. S. *J. Chem. Phys.* **1995**, 103, 7983.
- Becke, A. D. *J. Chem. Phys.* **1993**, 98, 5648.
- Lee, C.; Yang, W.; Parr, R. G. *Phys. Rev. B* **1988**, 37, 785.
- Hehre, W. J.; Radom, P.; Schleyer, P. v. R.; Pople, J. A. *Ab Initio Molecular Orbital Theory*; Wiley & Sons: New York, 1986.
- Frisch, M. J.; Trucks, G. W.; Schlegel, H. B.; Robb, M. A.; Cheeseman, J. R.; Zakrzewski, V. G.; Montgomery, J. A.; Stratmann, R. E.; Burant, J. C.; Dapprich, S.; Millam, J. M.; Daniels, A. D.; Kudin, K. N.; Strain, M. C.; Farkas, O.; Tomasi, J.; Barone, V.; Cossi, M.; Cammi, R.; Mennucci, B.; Pomelli, C.; Adamo, C.; Clifford, S.; Ochterski, J.; Petersson, G. A.; Ayala, P. Y.; Cui, Q.; Morokuma, K.; Malick, D. K.; Rabuck, A. D.; Raghavachari, K.; Foresman, J. B.; Cioslowski, J.; Ortiz, J. V.; Stefanov, B. B.; Liu, G.; Liashenko, A.; Piskorz, P.; Komaromi, I.; Gomperts, R.; Martin, R. L.; Fox, D. J.; Keith, T.; Al-Laham, M. A.; Peng, C. Y.; Nanayakkara, A.; Gonzalez, C.; Challacombe, M.; Gill, P. M. W.; Johnson, B.; Chen, W.; Wong, M. W.; Andres, J. L.; Gonzalez, C.; Head-Gordon, M.; Replogle, E. S.; Pople, J. A. *Gaussian 98, Revision A. 5*, Gaussian, Inc., Pittsburgh, PA, 1998.
- Melissas, V. S.; Truhlar, D. G.; Garrett, B. C. *J. Chem. Phys.* **1992**, 96, 5758.
- Truhlar, D. G.; Garrett, B. C. *Acc. Chem. Res.* **1980**, 13, 440.
- Fukui, K. *Acc. Chem. Res.* **1981**, 14, 363.
- Gonzalez, C.; Schlegel, H. B. *J. Chem. Phys.* **1989**, 90, 2154.
- Gonzalez, C.; Schlegel, H. B. *J. Phys. Chem.* **1990**, 94, 5523.
- Warburton, P.; Walker, P. D.; Mezey, P. G. *Rhocalc2000* program, Mathematical Chemistry Research, University of Saskatchewan, **2000**.
- Brickmann, J.; Keil, M.; Exner, T. E.; Marhöfer, R. *J. Mol. Mod.* **2000**, 6, 328.
- Waldherr-Teschner, M.; Goetze, T.; Heiden, W.; Knoblauch, M.; Vollhardt, H.; Brickmann, J. *MOLCAD – Computer Aides Visualization and Manipulation of Models in Molecular Science*; Second Eurographics Workshop on Visualization in Scientific Computing, Delft, Netherlands, 1991.
- Brickmann, J.; Keil, M.; Exner, T. E.; Marhöfer, R.; Moeckel, G. *The Encyclopedia of Computation Chemistry*; Schleyer, P. v. R., Allinger, N. C., Clark, T., Gasteiger, J., Kollmann, P. A., Schaefer III, H. F., Schreiner, P. R., Eds.; John Wiley & Sons: Chichester, 1998; p 1679.
- SYBYL 6.7, Tripos Inc., 1699 South Hamley Road, St. Louis, MO 63144, 2000.
- Walker, T. E. H.; Dehmer, P. M.; Berkowitz, J. *J. Chem. Phys.* **1973**, 59, 4292.
- Mezey, P. G. *Shape in Chemistry: Introduction to Molecular Shape and Topology*; VCH Publishers: New York **1992**.
- Mezey, P. G. *Int. J. Quantum Chem. Quantum Biol. Symp.* **1986**, 12, 113.
- Mezey, P. G. *J. Comput. Chem.* **1987**, 8, 462.
- Mezey, P. G. *Int. J. Quantum Chem. Quantum Biol. Symp.* **1986**, 14, 127.
- Mezey, P. G. *J. Math. Chem.* **1988**, 2, 299.
- Mezey, P. G. *J. Math. Chem.* **1988**, 2, 325.